UDC 539.2

STRUCTURE AND DIELECTRIC PROPERTIES OF NANOCOMPOSITES: OPAL MATRIX – TITANIUM OXIDE AND RARE-EARTH TITANATES*

M.I. Samoylovich[1], A.F. Belyanin[1,@], A.S. Bagdasaryan[2], V. Bovtun[3]

[1]*CRTI «Technomash», Moscow, Russia*
[2]*SEC «Technological developments of telecommunication and radio frequency identification», Moscow, Russia*
[3]*Institute of Physics ASCR, Praha, Czech Republic*
[@] *Corresponding author e-mail: belyanin@cnititm.ru*

The conditions for the formation of nanocomposites based on the basis of lattice packings SiO_2 nanospheres (opal matrices) with included clusters of crystalline phase of titanium oxide (TiO_2 and TiO) and rare-earth titanates of the general formula R_2TiO_5 or $R_2Ti_2O_7$, where R – Er, Dy, Gd, Pr, Tb and Yb in interspherical nanospacing are considered. The composition and structure of the nanocomposites were studied by electron microscopy, X-ray diffraction and Raman spectroscopy. Results of measuring of the frequency dependences of real and imaginary components of the permittivity and microwave conductivity (ranging 10^{-2}–10^{12} Hz) obtained nanostructures are viewed.

Keywords: *opal matrix, nanocomposites, titanium oxide, rare-earth titanates, X-ray diffractometry, Raman spectroscopy, dielectric properties.*

Introduction

Nanocomposites based on opal matrixes, the interspherical cavities of which are filled with various substances (ordered *3D* nanolattices of crystallites), are among new types of metamaterials. In turn, metamaterials based on opal matrixes are perspective in electronic equipment for creating devices controlling phase rates in the optical, ultra-high frequency and terahertz ranges [1, 2], various solid-state microwave devices (filters, delay lines, phase-shifting elements, etc.), and also sources of directed X-ray radiation and acoustic waves [3, 4].

Opal matrixes, i.e., three-dimensional three-layered cubic compositions based on latticed packing of nanospheres of X-ray amorphous SiO_2 with a diameter of 200–350 nm [5] with the interspherical cavities filled by titanium oxides or rare-earth element (REE) titanates, are of special practical interest. Thus, titanium dioxide is one of the most widely studied photocatalytic large-gap semiconductor materials, the photoelectrochemical activity of which strongly depends on the phase composition (crystalline and amorphous phases of TiO_2) [6]. The ranges of use of various titanium monoxide (TiO) phases can be shown as a result of stabilization of the phase under normal conditions, particularly, in the course of synthesis under the conditions of limited geometry of interspherical cavities of opal matrixes.

* Original Russian Text © M.I. Samoylovich, A.F. Belyanin, A.S. Bagdasaryan, V. Bovtun, 2016, published in Tonkie Khimicheskie Tekhnologii /Fine Chemical Technologies, 2016, Vol. 11, No 2, pp. 66–73.

Perspective substances for filling the interspherical cavities of opal matrixes are also such multiferroics as titanates, for example, dititanates $R_2Ti_2O_7$ (R = REE) having high melting temperatures and ferroelectric properties. Multiferroics can be used for producing elements of devices mutually transforming magnetic and electric signals. This property is due to the strong magnetoelectric effect observed for a number of compounds, for example, for a large class of titanium dioxides. REE dititanates are known, the anti-ferromagnetic, magnetic and ferroelectric properties of which coexist at low temperatures. As a result, they can serve as magnetic carriers and magnetic sensors [7, 8]. Antiferromagnetic properties are found for $Er_2Ti_2O_7$, $Dy_2Ti_2O_7$, $Yb_2Ti_2O_7$ and $Ho_2Ti_2O_7$ (so-called "frustrated" materials) [9].

Synthesis in the closed nanosized volume of interspherical cavities of opal matrixes promotes stabilizing high-temperature phases at low temperatures and decreasing the formation temperature of the synthesized substance.

The purpose of this work is to establish the influence of preparation conditions on the composition and dielectric properties of nanocomposites based on opal matrixes, in the interspherical cavities of which crystalline titanium oxides (TiO and TiO_2) and REE titanates having the formula R_2TiO_5 (oxotitanates) or $R_2Ti_2O_7$ (dititanates), where R = REE, are synthesized (Er_2TiO_5, $Dy_2Ti_2O_7$, $Gd_2Ti_2O_7$, $Pr_2Ti_2O_7$, $Tb_2Ti_2O_7$, $Yb_2Ti_2O_7$).

Experimental

Opal matrixes were obtained by the hydrolysis of orthosilicic acid tetraester with an ethanol solution in the presence of ammonium hydroxide as described in work [5].[1] Regularity of SiO_2 nanospheres packing was attained by their self-assembly (Figure 1a, b; scanning electron microscope (SEM) produced by CARL ZEISS LEO 1430 *VP* and atomic-force microscope (AFM) produced by Digital Instruments, Nanoscope 3).

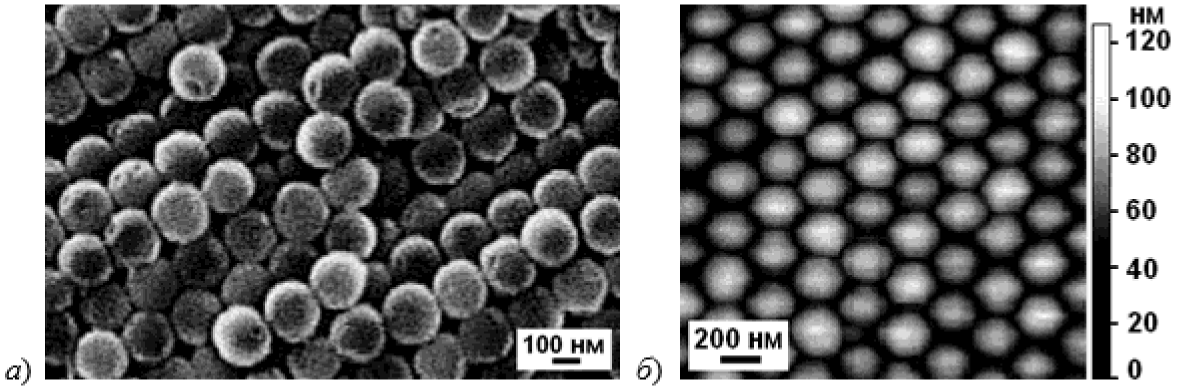

Figure 1. Structure (*a* – SEM; *b* – AFM) of the surface of the formation of opal matrixes samples (latticed packing of SiO_2 nanospheres).
[*а), б)* means *a), b)*; нм means nm]

---

[1] Hereinafter we mention reagents used for synthesizing the opal matrixes and samples of the nanocomposites. All the reagents were produced by Aldrich and Sigma.

Figure 2*a* shows three layers *1–3* of the closest cubic latticed packing of SiO_2 nanospheres *4*. Each nanosphere *A* in a flat densest layer is surrounded with six triangular gaps of various orientation (*B* and *C*). The upper layer of the nanospheres can be oriented with respect to the lower one either by positions *B* or by positions *C*. Under the conditions used in this work, a three-layered (cubic) composition *.../ABC/...* [5] was formed. The structure corresponds to the closest packing with the fill factor for the SiO_2 nanospheres equal to 74.05% [10]. The closest packing of the nanospheres forms tetrahedral and octahedral interspherical cavities, the volume of which is 25.95% of the volume of the opal matrixes conditionally consisting of spheres *10* and *11* (Figure 2,b) inscribed in the cavities and of the space connecting them. The diameters of the spheres inscribed in the tetrahedral and octahedral cavities are equal to ~ 0.22d and ~ 0.41d, respectively (*d* is the diameter of the SiO_2 nanospheres). The spheres inscribed in the interspherical cavities occupy 6.94% of the opal matrixes volume.

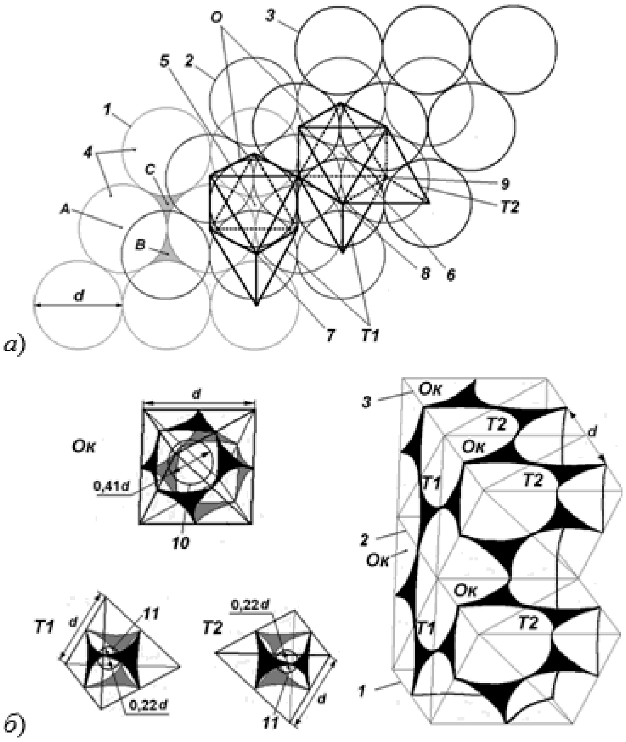

Figure 2. *a*) The structure of three (*1–3*) closely packed layers of SiO_2 nanospheres (*4*) of diameter *d* (projection to the plane {111}; the centers of the SiO_2 nanospheres form a face-centered cubic lattice) forming octahedral (*5, 6*) and tetrahedral (*7, 8* and *9*) cavities. *b*) Octahedrons (Oc) and tetrahedrons (*T1* and *T2*) formed by the SiO_2 nanospheres (*10* and *11* are spheres inscribed in octahedral and tetrahedral cavities) and the volume model of a substance filling the interspherical cavities of three (*1–3*) closely packed layers of the SiO_2 nanospheres.
[*a), б)* means *a), b)*]

Cavities *5* and *7* shown in Figure 2,*a* are created by the SiO_2 nanospheres of the first and second layers, and cavities *6*, *8* and *9* – by the second and third layers of the nanospheres closest packing. Connecting the centers of six and four nanospheres forming the cavities we obtain, respectively, octahedrons (Oc) and variously oriented tetrahedrons (T1 and T2) (Figure 2,*a*). The octahedrons and tetrahedrons completely fill the space. The interspherical cavities at the joint of the tetrahedrons and octahedrons (shown in Figure 2,*b*) have the maximum size of 0.37*d*. The interspherical tetrahedral and octahedral cavities can be filled with various substances. Figure 2 shows the volume model of a substance that filled ten interspherical cavities (four octahedral and six tetrahedral ones). The cavities are located in the three-layered packing.

In order to form nanocomposites samples of opal matrixes 2–3 cm^3 in volume with the sizes of monodomain areas ≥ 0.1 mm^3 and a SiO_2 nanospheres diameter of ~ 260 nm were used. The interspherical cavities of the opal matrixes were filled with titanium oxides and REE titanates also by the method of impregnation [5].

Nanocomposites based on the opal matrixes, the interspherical cavities of which were filled with the REE titanates (Er_2TiO_5, $Dy_2Ti_2O_7$, $Gd_2Ti_2O_7$, $Pr_2Ti_2O_7$, $Tb_2Ti_2O_7$, $Yb_2Ti_2O_7$), were obtained by the introduction of REE nitrates into a 15% solution of $TiCl_3$ in a low-concentrated solution of hydrochloric acid (HCl). The impregnation was carried out 6–10 times with subsequent low-temperature heat treatment at 300–500°C. Then the opal matrixes with the introduced substances were subjected to heat treatment in the air at 800–1000°C. The synthesized substances filled 40–60% of the volume of the interspherical cavities of the opal matrixes.

Nanocomposites based on the opal matrixes, the interspherical cavities of which were filled with titanium oxides, were obtained by the introduction of a 15% solution of $TiCl_3$ in diluted HCl into the interspherical cavities of the opal matrixes followed by heat treatment. The cavities filling with the solution and preliminary heat treatment at 300–400°C were carried out 8 times. The crystalline phase of TiO_2 was formed by heat treatment of the nanocomposites in the air at 700–1000°C, and that of TiO – by heat treatment in hydrogen. The heat treatment in a flow of hydrogen was carried out with the use of an Otzhig TM−6 installation (developed in the Scientific Research Institute of Precision Engineering, Zelenograd) ensuring automatic operation of the heating chamber according to a preset program. The following parameters were used for the high-temperature heat treatment when obtaining the nanocomposites containing TiO: a preliminary purge of the reactionary chamber with a chemically inert gas (N_2 or Ar) for 20 min; heating at a rate of 600 °C/h in a hydrogen stream (at a pressure of 5 atm); temperature of processing in H_2: 1000°C (2 h at a hydrogen pressure of 3–5 atm). This method was used to obtain nanocomposites, the interspherical cavities of which are filled with TiO_2 or TiO crystallites by 30–40%.

In order to identify the crystalline phases of the compounds synthesized in the interspherical cavities X-ray diffractometers *ARL* X'tra и *XRD*-6000 were used (Cu *k*α radiation, an energy-dispersive solid-state detector with a Peltier cooler, a graphite monochromator, no sample rotation, incrementation parameter 0.01°C/min, continuous mode 1°C/min). The X-ray patterns were analyzed with the use of an automated *ICDD PDF*-2 database.

Results and Discussion

<u>*X-Ray diffractometry.*</u> The X-ray phase analysis of samples of the nanocomposites containing REE titanates allowed to establish the presence of the following crystalline phases: $Gd_2Ti_2O_7$; $Tb_2Ti_2O_7$; $Dy_2Ti_2O_7$; $Yb_2Ti_2O_7$ (all of them are of the cubic syngony, spatial group *Fd*3*m*); $Pr_2Ti_2O_7$ (monoclinic syngony, $P2_1$); Er_2TiO_5 (hexagonal syngony), and also various titanium oxides (in the largest quantities): TiO_2-rutile (tetragonal syngony, $P4_2/mnm$); $Ti_{0.72}O_2$-anatase (tetragonal syngony, $I4_1/amd$).

X-ray patterns of the opal matrixes containing the crystalline phases Er_2TiO_5 and $Dy_2Ti_2O_7$ are presented in Figure 3.

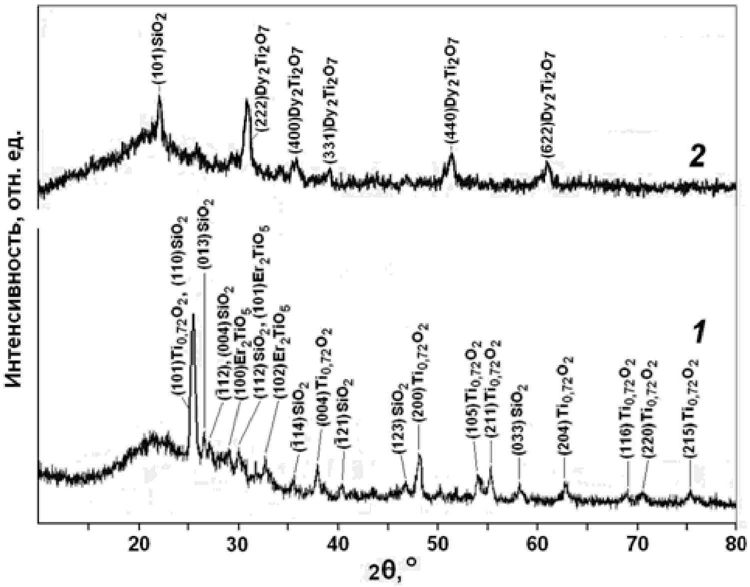

Figure 3. X-Ray patterns of samples of the opal matrixes, the interspherical cavities of which contain crystallites of Er_2TiO_5 (1) and $Dy_2Ti_2O_7$ (2).
[Интенсивность, отн. ед. means Intensity, rel. units]

X-ray patterns of samples of the opal matrixes, the interspherical cavities of which are filled with titanium oxides, are presented in Figure 4. The presence of the following crystalline phases was established: TiO_2-rutile (tetragonal syngony, $P4_2/mnm$) and TiO (cubic syngony, *Fm*-3*m*).

Note that, when carrying out the synthesis in the closed nanosized volume (the interspherical cavities of the opal matrixes were used for this purpose), the composition and structure of the substances significantly differ from the results of synthesizing bulk samples. The obtained data can be the result of the synthesis under restricted sizes of the crystallites (the process of growth or recrystallization under the conditions of limited geometry of the crystallizer).

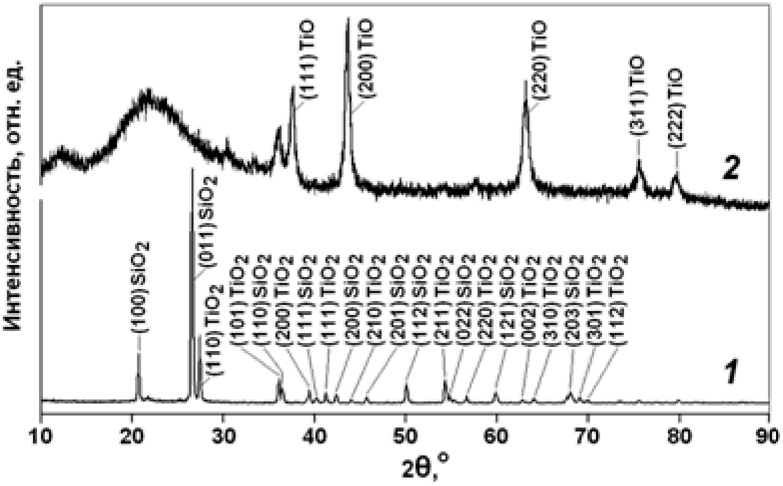

Figure 4. X-Ray patterns of samples of the opal matrixes with TiO_2-rutile (1) and TiO (2) crystallites synthesized in the interspherical cavities.
[Интенсивность, отн. ед. means Intensity, rel. units]

High-temperature heat treatment of the samples is followed by the formation of SiO_2 crystalline phases in small concentrations. In the samples of REE titanates synthesized at temperatures ≥800°C the presence of three crystalline phases of silicon dioxide is established: SiO_2-christobalite (tetragonal syngony, $P4_12_12$); SiO_2-tridymite (hexagonal syngony, $P6_3/mmc$) and SiO_2 (monoclinic syngony, $I2/a$). When synthesizing titanium dioxides, a SiO_2 crystalline phase (quartz, hexagonal syngony, $P3_12_1$) is formed (Figure 4, diffractogram 1). High-temperature heat treatment in the atmosphere of H_2 does not result in the formation of SiO_2 crystalline phases.

The size of the crystallites (areas of coherent scattering of X-ray radiation) in the synthesized substances calculated by the broadening of diffraction maxima in the X-ray patterns is equal to 49.0–59.8 nm for the TiO_2-rutile phase, 15.8–18.0 nm for TiO and 16–36 nm for the REE titanates. The specified sizes are less than the diameters of the spheres inscribed in the tetrahedral and octahedral cavities of the opal matrixes equal to 57.2 nm (0.22*d*) and 106.6 nm (0.41*d*), respectively.

The structure of the opal matrixes with the titanium oxides synthesized in the interspherical cavities was studied by transmission electronic microscopy (TEM) with the use of the particle size reduction technique allowing to separate the SiO_2 nanospheres and the particles of the synthesized substance (Figure 5; electronic microscope of *JEM* 200*C*). The particles of the synthesized substances had almost the equiaxial shape of crystallites. The synthesis temperature within the range 700–1000°C does not affect the size and shape of the crystallites of titanium oxides. The synthesized REE titanates and titanium oxides did not interact with the SiO_2 nanospheres. The size of the particles of the synthesized substance seen with the use of TEM (~ 20–30 nm for TiO and ~ 25–90 nm for the TiO_2-rutile phase) corresponds to the size of the crystallites calculated according to the X-ray diffractogram.

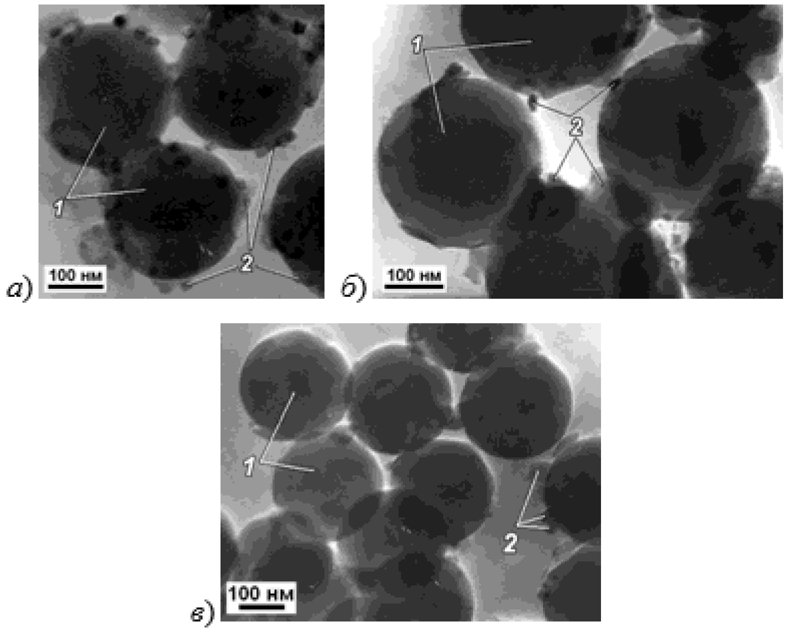

Figure 5. The structure (TEM) of SiO_2 nanospheres (1) of the opal matrixes and of the crystallites synthesized in their interspherical cavities (2): *a*) TiO; *b*) TiO_2-rutile; *c*) mixtures of titanium oxides. [*а), б), в)* means *a), b), c)*; нм means nm]

Raman scattering (RS) spectroscopy. X-Ray diffractometry is not sensitive to phases with crystallite sizes <1 nm, which maintain the functional properties of the synthesized materials. At the same time RS spectroscopy gives a chance to analyze the materials both in the crystalline and in the X-ray amorphous states. RS spectra were registered with the use of a laser microraman LabRAM *HR*800 spectrometer (HORIBA Jobin-Yvon) (632.8 nm He-Ne laser line; laser power <300 mW; beam spot diameter ~ 4 μm^2; analyzed layer depth ~ 3 μm).

RS spectra of the nanocomposites containing titanium oxide crystallites are presented in Figure 6, curves *1, 2*. In the RS spectra, the thermodynamically stable phase, TiO_2-rutile, has the base bands in the range $\Delta\nu$ equal to 462 and 622 cm^{-1} (bands broadening $\Delta\nu_{1/2}\approx 36.9$ and 39.5 cm^{-1}, respectively) and low intensity bands at $\Delta\nu$ 235, 295 and 703 cm^{-1}. The bands of the crystalline TiO_2-rutile phase are observed after heat treatment of an X-ray amorphous sample at 400 °C and above, their intensity increasing as temperature rises due to the increase of the crystallinity degree of the TiO_2-rutile phase. The X-ray amorphous TiO_2 is mainly transformed into TiO_2-anatase at a temperature ~ 400 °C. Changes in the position of the bands in the RS spectrum of the nanostructured TiO_2-anatase and TiO_2-rutile phases can be caused by composition deviations from stoichiometry. The bands in the RS spectrum at $\Delta\nu$ equal to 246–272 and 1077–1170 cm^{-1} are attributed to SiO_2 phases of various modifications: christobalite, tridymite and α-quartz.

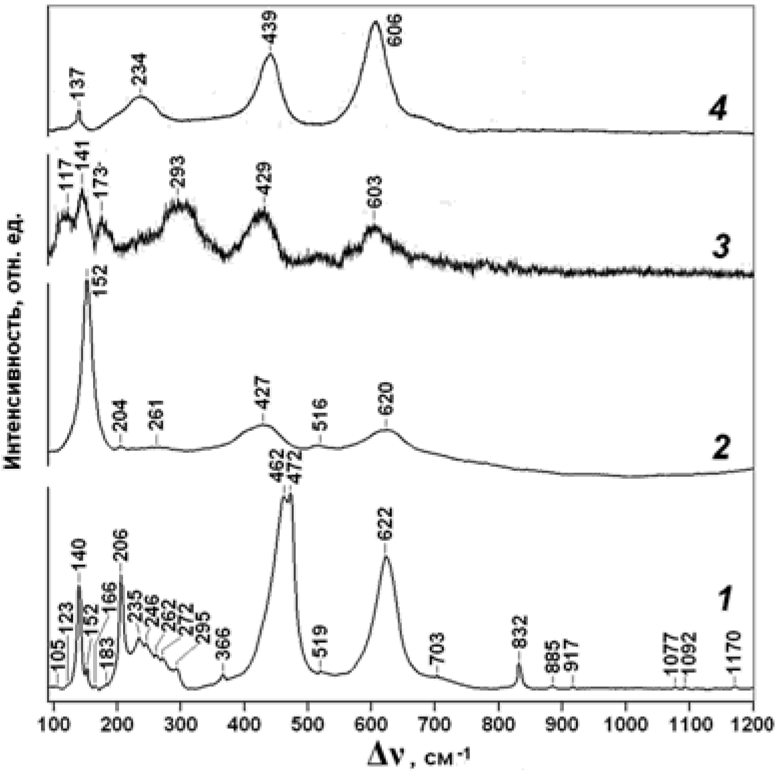

Figure 6. RS spectra of the samples of the opal matrixes, the interspherical cavities of which are filled with crystallites: TiO_2-rutile (*1*), TiO (*2*), $Dy_2Ti_2O_7$ (*3*) and $Yb_2Ti_2O_7$ (*4*). [Интенсивность, отн. ед. means Intensity, rel. units; $см^{-1}$ means cm^{-1}]

The RS spectrum of the nanocomposite containing TiO is presented in Figure 6 (spectrum *2*). The RS spectra of the samples of opal matrixes, the interspherical cavities of which are filled with TiO, have bands relating to the TiO_2-rutile and TiO_2-anatase phases. The broadening of the spectral bands of titanium oxides is due to the small sizes of the phase crystallites of the synthesized oxides. As the synthesis temperature rises, $\Delta\nu_{1/2}$ in the RS spectra of the samples increases, while the position of the bands shows oppositely directed dependence.

The RS spectra of the samples of REE titanates prepared at temperatures ≤700°C show that a multiphase X-ray amorphous substance is formed in the interspherical cavities. The RS spectra of the samples of the nanocomposites containing crystallites of REE titanates

($Dy_2Ti_2O_7$ and $Yb_2Ti_2O_7$) synthesized at temperatures > 800°C are presented in Figure 6 (curves *3* and *4*). The RS spectra have bands typical of the crystalline phases of REE titanates filling interspherical cavities, and also of the X-ray amorphous REE oxides and crystalline phases of titanium oxide [11, 12].

Dielectric characteristics. The real (ε′) and imaginary (ε″) parts of permittivity in the range of frequencies 10^6–$1.8{\cdot}10^9$ Hz were measured with the use of a Novocontrol *BDS* 2100 dielectric spectrometer with a coaxial measuring cell and an impedance Agilent 4291*B* analyzer. The measuring equipment produced by Agilent contained a component for measuring dielectric and magnetic permittivity, including losses, in the range 10 MHz – 110 GHz. Measurements in the microwave area ($2{\cdot}10^8$–$2{\cdot}10^{10}$ Hz) were made by the method of coaxial probe with the open end (Agilent 8507*E*) with the use of an Agilent *E*8364*B* network analyzer. In the terahertz range the measurement was performed by the method of transmission THz spectroscopy with a femtosecond Ti-sapphire laser system. The coaxial measurements ($1{\cdot}10^6$–$1.8{\cdot}10^9$ Hz) were carried out with the use of cylinder-shaped samples (diameter of 3 mm, height of 4–5 mm). All the other measurements were performed with the use of plate-shaped samples (10×10 mm, 1–3 mm thick). The estimation of the parameters of the real (ε′) and imaginary (ε″) parts of permittivity was carried out with the use of the auxiliary program superlattice0000_04_my.m.

The frequency dependences of ε′ and ε" a component of dielectric permeability (in the range of frequencies of 10^6–10^{12} Hz) for the opal matrixes with the crystallites of REE titanates synthesized in the interspherical cavities ($Yb_2Ti_2O_7$ and Er_2TiO_5) were studied. The results of the measurements are summarized in Figure 7. The measurements were carried out with the use of samples without electroding. Dielectric dispersion of frequencies in the microwave range is feebly marked. It was found that the permittivity of opal matrixes ε′, the interspherical cavities of which are filled with REE titanates, is higher than that of opal matrixes without filling. It was shown that in case of the studied nanocomposites dielectric losses increase both towards low frequencies (f<10 MHz) and towards high frequencies (closer to THz): the increase of low-frequency ε′ losses is caused by direct current conductance, and that of high-frequency is due to ε′ dispersion.

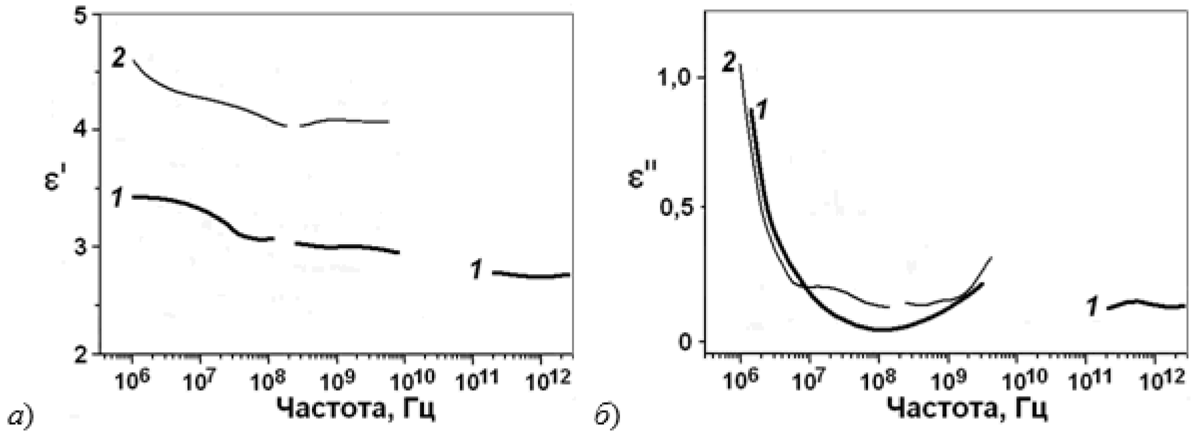

Figure 7. Frequency dependences of the real (*a*) and imaginary (*b*) parts of permittivity in the range of frequencies 10^6–$1.8\cdot10^9$ Hz for the samples of the opal matrixes, the interspherical cavities of which are filled with crystallites $Yb_2Ti_2O_7$ (*1*) and Er_2TiO_5 (*2*).
[*а), б)* means *a), b)*; Частота, Гц means Frequency, Hz]

The frequency dependences of the real (ε′) and imaginary (ε") parts of permittivity, as well as of conductivity (σ) of the opal matrixes, the interspherical cavities of which are filled with the TiO_2-rutile and TiO crystallites synthesized at 1000°C were studied (Figures 8, 9).

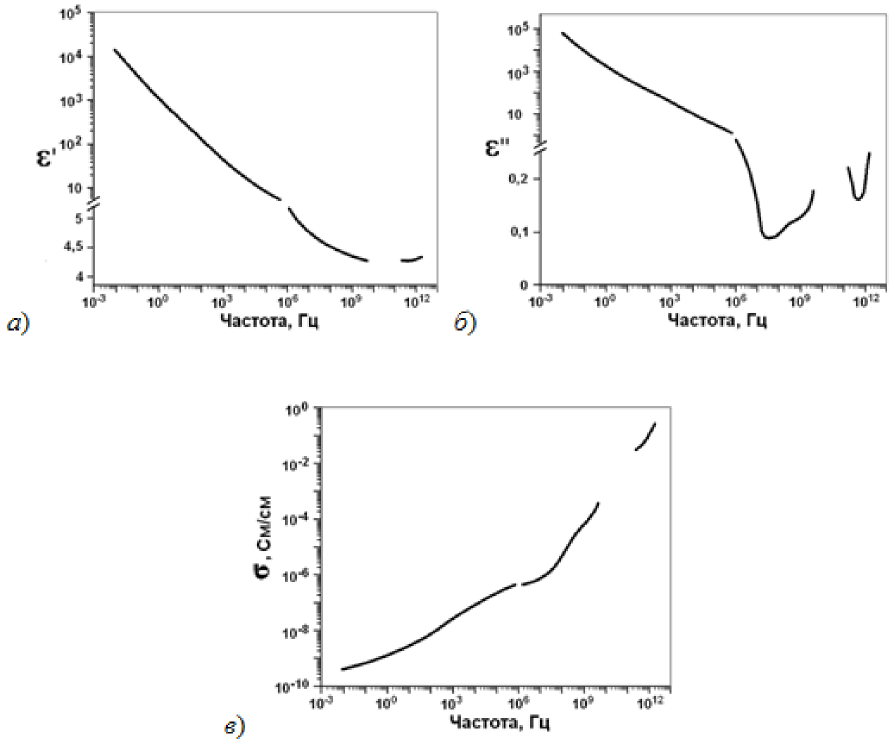

Рис. 8. Frequency dependences of the real (*a*) and imaginary (*b*) parts of permittivity and of microwave conductivity (*c*) of the opal matrixes, the interspherical cavities of which are filled with TiO_2-rutile crystallites.
[*а), б), в)* means *a), b), c)*; a, b, c;
Частота, Гц means Frequency, Hz;
σ, См/см means σ, Cm/cm]

Figure 8 presents the results of measurements of a sample containing (according to X-ray phase analysis and RS spectroscopy) crystallites of the TiO_2-rutile phase and X-ray amorphous phases of titanium oxides. The shape of the frequency dependence curves for the permittivity and conductivity of the nanocomposites containing TiO is similar to the results obtained for the nanocomposites containing the TiO_2-rutile phase presented in Figure 8. Introducing titanium oxide crystallites leads to an increase in ε' of the opal matrixes by 40–200%, but does not influence the dielectric losses: they remain low ($\varepsilon'' < 0.1$) in the whole used frequency range. There is a small increase of the dielectric losses in the low frequency range (~ 10^6 Hz) and their growth in the high frequency range (10^{10}–10^{12} Hz). The growth of the losses in the THz range, obviously, is caused by the low-frequency wing of the phonon spectrum of the introduced compounds.

The samples of the opal matrixes, the interspherical cavities of which are filled with titanium oxide crystallites, have a very small direct current conductance. This is clearly indicated by the low-frequency plateau of $\sigma(f)$ dependence that is of most likely due to surface leakage currents and to the presence of the X-ray amorphous phases. The dielectric permeability ε' of the studied opal matrixes, the cavities of which are filled with TiO_2 and TiO crystallites, is higher than the ε' values of the unfilled opal matrix. The whole specified frequency range shows dielectric dispersion typical of composite materials. The ε' values slightly decrease with frequency. At the same time, dielectric losses increase both towards low frequencies ($f < 10$ MHz) and towards THz frequencies.

The study of the effects of the electric field on the above dependences in the frequency range 1–10^6 Hz was carried out with the use of nanocomposite samples containing TiO (Figure 9). The measured dependencies of the shift on the electric field (at 300°K) for such a sample showed a low direct current conductance and a weak dependence on the displacement fields at low frequencies. The studied materials are so-called "bad" dielectrics with high losses and the strong relaxational polarization, and their characteristics (losses and conductivity at high frequencies) differ just a little from the parameters of the unfilled opal matrixes. The nonlinearity is almost not noticeable at the frequency of 1 kHz, and at 1 Hz e', e'' and σ slightly decrease with increasing field intensity (Figure 9).

In our opinion, the weak nonlinearity attests that the large low-frequency decreases in e', ε'' and σ are not caused by processes at the electrode, but are due to relaxation polarization (or due to the existence of hopping conductivity) of the nanocomposite. The main contribution is made by titanium oxides synthesized in the interspherical cavities of the opal matrixes. The applied field mainly affects the opal matrix (SiO_2). The latter is not electrically active and has no significant conductivity or dielectric nonlinearity. The formation of the crystalline phases of SiO_2 occurs from the nanospheres surface, and the structure and concentration of the crystalline phases of SiO_2, in turn, depend on the heat treatment conditions.

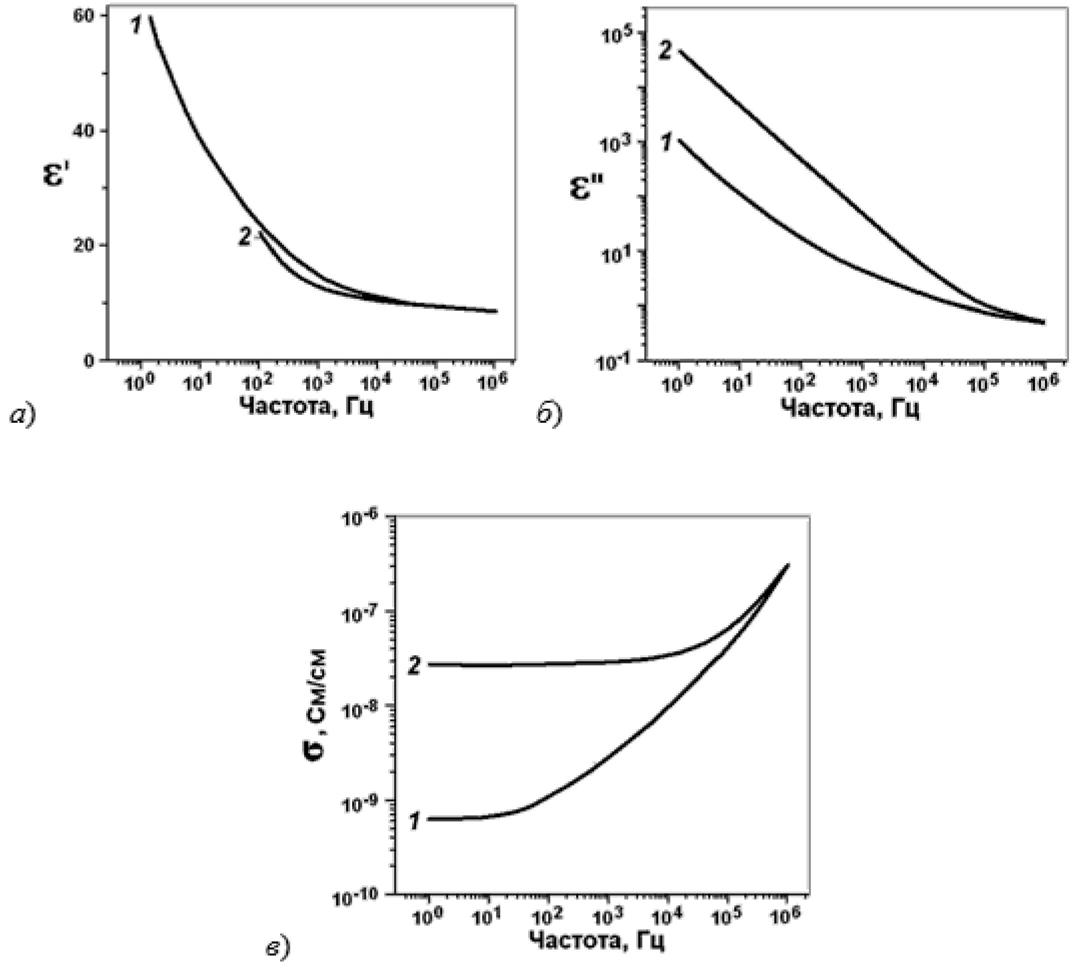

Figure 9. Frequency dependences of the real (*a*) and imaginary (*b*) parts of permittivity, and also of microwave conductivity (*c*) of the samples of the opal matrixes, the interspherical cavities of which are filled with TiO crystallites: 1) without applied field; 2) upon applying a 100 V field. [*а), б), в)* means *a), b), c)*; a, b, c; Частота, Гц means Frequency, Hz; σ, См/см means σ, Cm/cm]

All the materials have the properties of ceramic type composites with the concentration of the conducting filler slightly higher than the percolation threshold. The weak percolation is also indicated by the low level of low-frequency conductance and, as a result, of direct current conductance. The measured spectra of the frequency dependence of conductance and of permittivity parameters show that the studied samples are materials that passed the percolation threshold for the introduced components.

Conclusion

Samples of opal matrixes ($3D$-latticed packings of SiO_2 nanospheres ~ 260 nm in diameter) with a volume of 2–3 cm^3, with the sizes of monodomain areas up to 0.1 of mm^3 were obtained. Ordered $3D$ nanolattices of crystallites of titanium oxides (TiO_2 and TiO) and of REE titanates (Er_2TiO_5, $Dy_2Ti_2O_7$, $Gd_2Ti_2O_7$, $Pr_2Ti_2O_7$, $Tb_2Ti_2O_7$, $Yb_2Ti_2O_7$). based on the opal matrixes with filled interspherical cavities were prepared. The specific features of crystallization and phase transformations in the interspherical cavities of the opal matrixes of the above substances were studied. The formation of the low titanium oxide (TiO) in the interspherical cavities of the opal matrixes was attained by controlled high-temperature heat treatment in hydrogen. The crystallites of the REE titanates synthesized in the interspherical cavities had the sizes 16–36 nm, and those of titanium oxides, 490–59.8 nm for TiO_2 and 15.8–18.0 nm for TiO.

The frequency dependencies of the real and imaginary parts of permittivity were measured, as well as those of conductivity in the range 10^{-2}–10^{12} Hz. The increased values of permittivity of the opal matrixes, the interspherical cavities of which are filled with crystallites of REE titanates (Er_2TiO_5 and $Yb_2Ti_2O_7$) upon preservation of low losses in the microwave range account for the interest in the studied composites as a stage of the search and subsequent creation of new metamaterials. Understanding the features of the phase transformations and crystallization in the interspherical cavities of the opal matrixes allows creating metamaterials with controlled values of the functional properties and operational characteristics.

An interrelation between the microwave characteristics and the phase composition of titanium oxides and REE titanates was established. Besides, data required for using such non-crystalline non-uniform materials with spatial modulation (dispersion) of the electric and dielectric parameters in the nanometer range were obtained. It is supposed that the approach applying such nanocomposites will be most effective when developing various solid-state microwave devices: filters, delay lines and other controlling elements.

The work was performed with support of the Russian Foundation for Basic Research (grant 15-07-00529 A).

References:

1. Sarychev A.K., Shalaev V.M. Electrodynamics of metamaterials. World Scientific and Imperial College Press, 2007. 200 p. doi: 10.1142/9789812790996.

2. Kong J.A. // Progress in Electromagnetics Research, PIER. 2002. V. 35. P. 1–52.

3. Tchernega N.V., Samoylovich M.I., Belyanin A.F., Kudryavtseva A.D., Kleshcheva S.M. // Nano- i mikrosistemnaya tekhnika (Journal of Nano and Microsystem Technique). 2011. № 4. P. 21–31. (in Russ.)

4. Tcherniega N.V., Samoilovich M.I., Kudryavtseva A.D., Belyanin A.F., Pashchenko P.V., Dzbanovski N.N. // Optics Letters. 2010. V. 35. № 3. P. 300–302.

5. Samoylovich M.I., Kleshcheva S.M., Belyanin A.F., Zpitkovskij V.D., Tsvetkov M.Yu. // Nano- i mikrosistemnaya tekhnika (Journal of Nano and Microsystem Technique). 2004. № 6. P. 3–7. (in Russ.)

6. Hardcastle F.D. // J. Arkansas Academy of Science. 2011. V. 65. P. 43–48.

7. Kimura T., Goto T., Shintani H., Ishizaka K., Amira T., Tokura Y. // Nature. 2003. V. 426. P. 55–58.

8. Hill N.A. // J. Phys. Chem. B. 2000. V. 104(29). P. 6694–6709.

9. Bramwell S.T., Field M.N., Harris M.J., Ivan M.J. // J. Physics Condensed Matter. 1999. V. 2(4). P. 483–495. DOI: 10.1088/0953-8984/12/4/308.

10. Belov N.V. The structure of ionic crystals and metal phases. M.: Publ. of Academy of Sciences of USSR, 1947. 237 p. (in Russ.)

11. Samoylovich M.I., Belyanin A.F., Bagdasaryan A.S., Rinkevich A.B., Bagdasaryan S.A., Bovtun V. // Naukoyomkie tekhnologii (Science Intensive Technologies). 2015. V. 16. № 10. P. 65–71. (in Russ.)

12. Samoylovich M.I., Belyanin A.F., Bagdasaryan A.S., Rinkevich A.B., Bagdasaryan S.A., Bovtun V. // Nanoinzheneriya (Nanoengineering). 2015. № 11. P. 12–21. (in Russ.)